Progress In Electromagnetics Research Letters, Vol. 112, 59–65, 2023

On the Propagation through Annular Core Optical Fiber under DB Boundary Conditions

Muhammad Saqlain[1], Lway F. Abdulrazak[2], Muhammad Kashif[3], Talib A. Al-Sharify[4], Laith S. Ismail[5], and Muhammad A. Baqir [1, *]

Abstract—In this paper, we investigate the propagation behavior of electromagnetic waves through coaxial optical fiber bounded with DB-boundaries. For this purpose, an eigenvalue equation is derived by using suitable DB-boundary conditions to determine the allowed values of propagation constant β for each propagating mode. Moreover, we have analyzed the electric field and power distribution patterns through coaxial optical fiber for different propagating modes and dimensions, respectively. Our results show that small dimensional guide confinement remains maximum close to the lower interface of the guide, whereas, for larger dimensions, it shifts toward the upper interface. Investigations show that high power is confined by H_{12} mode compared to H_{11} mode, and, therefore, shows contrary behavior compared to commonly used fibers.

1. INTRODUCTION

The interaction of electromagnetic waves with objects depends on their material properties and geometrical structures. Some non-natural existing properties of the materials include negative reflection/refraction [1, 2], reversal of Doppler shift [3], and Cherenkov radiations [4] can be achieved by developing such structures and terms as metamaterials. These are the composition of periodically arranged small unit cells similar to atoms and molecules in the matter and support the backward wave phenomenon [5]. Further, several novel devices such as perfect lenses [6], cloaking devices [7], filters [8], oscillators [9], broadband antennas [10], and perfect absorber [11] have been developed by implementing these materials.

For a unique solution based on differential equations that express the electromagnetic field problems, boundary conditions with two scalar conditions are applied at the interface. For their representation, the tangential components of electromagnetic (EM) fields are involved. A recently reported work explains the type of boundary condition that involves the normal components of the fields and terms these DB boundary conditions [12–15]. Recently, Zaluski et al. experimentally realized the DB metasurface using a compact unit cell made of a small loop antenna and an LC-loaded dipole [16, 17]. Several studies present DB mediums-based structures [17–24]. Among them, the skew medium-based DB boundary [23] and the realization of the cloaking concept are explained in [24]. In this work, we analyze the propagation phenomenon of EM waves through the coaxial fiber with DB-boundary. The inner and outer boundaries of fiber are composed of DB mediums. It is worth noting that the normal components of electric and magnetic fields become zero at the interface of DB boundary. Here, we have investigated the electric

Received 4 April 2023, Accepted 14 July 2023, Scheduled 28 August 2023

* Corresponding author: Muhammad Abuzar Baqir (abuzar@cuisahiwal.edu.pk).

[1] Department of Electrical and Computer Engineering, COMSATS University Islamabad, Sahiwal, Pakistan. [2] Department of Computer Science, Cihan University Sulaimaniya, Sulaimaniya 46001, Kurdistan Region, Iraq. [3] Department of Electrical Engineering, Faculty of Engineering & Technology, Bahauddin Zakariya University, Multan Punjab, Pakistan. [4] Medical Laboratory Techniques, Al-Rafidain University College, Baghdad 10064, Iraq. [5] Computer Technologies Engineering, Al-Turath University College, Baghdad, Iraq.

field corresponding to two different lower-order hybrid modes and its power confinement due to the variation of radial dimensions of the guide. Moreover, the effect of the DB boundary on the dimensional parameters is one of the performance metrics for tailoring the confinement inside the guide. The remaining part of the paper is as follows. Section 2 incorporates the analytical treatment of the given structure. Section 3 introduces the results and discussion about energy and power distribution through coaxial fiber. Section 4 contains the conclusion part.

2. FORMULATION AND THEORY

Figure 1 shows the schematic of the annular core optical fiber under DB boundaries. The inner and outer boundaries of the DB medium are at $r = a$ and $r = b$ (as illustrated in Fig. 1). For the isotropic medium, the normal component of the electric and magnetic field vanishes at the interface of DB boundary, defined as [12, 19]

$$\hat{n} \cdot \mathbf{E} = 0 \tag{1}$$

$$\hat{n} \cdot \mathbf{H} = 0 \tag{2}$$

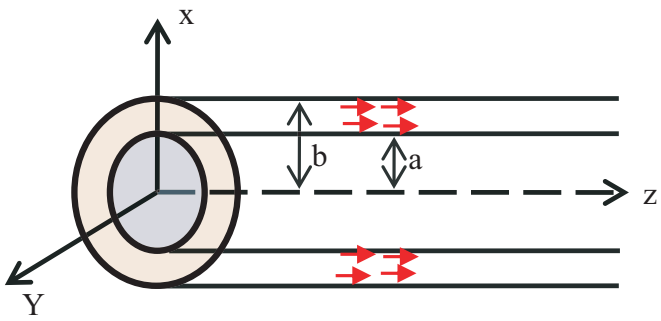

Figure 1. Schematic diagram of coaxial optical fiber.

In the proposed coaxial optical fiber, the field remains trapped in the region $a < r < b$. The eigenvalue equation is derived by applying the suitable boundary conditions at the DB interfaces, where $r = a$ and $r = b$ which results in a set of four homogeneous equations [19], and the corresponding characteristic equation is obtained as follows;

$$\begin{aligned} f(\beta) = {} & \frac{v^2\omega^2\mu\varepsilon}{b}\left\{\frac{4v^2\omega^2\mu\varepsilon J_v(ka)\,Y_v(kb)\,M_1}{4a^2b}\right. \\ & + \frac{k^4\beta^2a^2N_1Y_v(kb)\,(N_1Y_v(kb)+N_2J_v(kb))}{4a^2b} - \frac{4v^2\omega^2\mu\varepsilon J_v(kb)\,Y_v(kb)\,M_1}{4a^2b} \\ & + \frac{N_2k^2\beta^2a^2J_v(kb)\,(Y_v(kb)\,N_1+J_v(kb)\,N_2)}{4a^2b}\,\frac{k\beta Y_v(ka)\,N_1\,(\gamma_1Y_v(kb)+J_v(kb))}{4a^2} \\ & \left. + \frac{N_2J_v(ka)\,(M_1Y_v(kb)+M_1J_v(kb))}{4a^2}\right\} \\ & + \frac{k^4\beta^2}{4}\left\{\frac{4v^2\omega^2\mu\varepsilon Y_v(kb)\,\gamma M_1\,(M_1Y_v(ka)-M_2J_v(ka))}{4a^2} - \frac{k^4\beta^2a^2\eta_2\,(N_1M_1}{4a^2} - \frac{N_1M_1}{4a^2}\right) \\ & + \frac{v\omega\mu\varepsilon}{ab}\,(Y_v(ka)\,N_1\,(J_v(kb)M_1) - Y_v(kb)\,M_1) + J_v(ka)\,(Y_{v+1}(ka) - Y_{v-1}(ka))J_v(kb)\,(Y_{v-1}(kb) \\ & - Y_{v+1}(kb)) - M_1) + \frac{M_1}{4a^2}\left(4v^2\omega^2\mu\varepsilon\; J_v(ka)\,(J_v(ka) - M_1Y_v(ka)) + a^2k^4\beta^2\;N_1)^2\,\tau\right\} = 0 \end{aligned} \tag{3}$$

The symbols used in Equation (3) are defined as;

$$M_1 = J_v(ka)\,Y_v(kb) + J_v(kb)\,Y_v(ka) \tag{4a}$$

$$N_1 = (J_{v-1}(ka) - J_{v+1}(ka)) \tag{4b}$$

$$N_2 = (Y_{v-1}(ka) - Y_{v+1}(ka)) \tag{4c}$$

$$M_2 = (J_{v-1}(kb) - J_{v+1}(kb)) \tag{4d}$$
$$\tau = (Y_{v+1}(ka) - Y_{v-1}(ka)) \tag{4e}$$

Similarly, the unknown constants B_1, C_1, and D_1 can be evaluated in terms of A_1 and can be written as;

$$B_1 = -\frac{\beta kaS\Theta + \omega^2\mu\epsilon v^2 G\mathrm{L}}{\beta kaQ\Theta + \omega^2\mu\epsilon v^2 G\mathrm{L}} A_1 \tag{5a}$$

$$C_1 = \frac{\chi\left(\beta kaS\Theta + \omega^2\mu\varepsilon v^2 G\mathrm{L}\right) - \Delta\left(\beta kaQ\Theta + \omega^2\mu\varepsilon v^2 G\mathrm{L}\right)}{\beta ka\theta\left(\beta kaQ\Theta + \omega^2\mu\varepsilon v^2 GL\right)} A_1 \tag{5b}$$

$$D_1 = -\frac{\beta^2 k^2 a^2 \Theta\left(J'_v(ka) P_1 + Y'_v(ka) P_2\right) + jv\mu\omega J_v(ka)\left(\chi P_2 - \Delta P_1\right)}{jv\beta\mu\omega kaP_1} A_1 \tag{5c}$$

whereas,

$$P_1 = \beta kaQ\Theta + \omega^2\mu\epsilon v^2 \mathrm{GL} \tag{6a}$$
$$P_2 = \beta kaS\Theta + \omega^2\mu\epsilon v^2 \mathrm{GL} \tag{6b}$$
$$S = \left(\beta kbJ'_v(kb) - jv\mu\omega Y_v(kb)\right) \tag{6c}$$
$$\Theta = Y'_v(ka) - J'_v(ka) \tag{6d}$$
$$G = J_v(kb) - Y_v(kb) \tag{6e}$$
$$L = J_v(ka) + \beta aY'_v(ka) \tag{6f}$$
$$\mathrm{Z} = J_v(ka) + \beta aY_v(ka) \tag{6g}$$
$$Q = \beta kbY'_v(kb) - jv\mu\omega Y_v(kb) \tag{6h}$$
$$\chi = jv\omega\varepsilon Y_v(ka) + \beta kaY'_v(ka) \tag{6i}$$
$$\Delta = jv\omega\varepsilon J_v(ka) + Y'_v(ka) \tag{6j}$$

where the wavenumber $k = \sqrt{n^2k_o^2 - \beta^2}$, k_o and β are the free-space wavenumber and propagation constant, and refractive index of medium $n = 1.5$.

We can calculate the flux density through the core section of the coaxial optical fiber along the z-axis which can be written as [25];

$$S_z = \frac{1}{2}(E_r H^*_\varphi - E_\phi H^*_r) \tag{7}$$

The power through coaxial optical fiber can be determined as follows [26, 27];

$$P_z = \int_0^{2\pi}\int_a^b r.S_z dr d\phi \tag{8}$$

The numerical solution of Equation (8) can be obtained using a mathematical computation software tool called Mathematica. Further, the normalized electric field components and power distribution are considered and obtained by dividing the respective highest obtained values. Further, the normalized values of electric field components and power distribution are considered and obtained by dividing the respective highest obtained values.

3. RESULTS AND DISCUSSION

Now, we examine the electric field and power confinement in coaxial dielectric optical fiber. For the computation, the inner boundary of the optical fiber is kept fixed at $a = 2\,\mu\mathrm{m}$, and the operating wavelength $\lambda = 1.55\,\mu\mathrm{m}$. Firstly, we analyze the electric field behavior and then discuss the power distribution inside the guide. Within the context, the allowed values of propagation constant β are determined numerically from the eigenvalue Equation (3) and given in Table 1.

Table 1. Propagating constant β for each propagating mode when varying the outer radius of the given fiber.

Outer radius	Mode order	Propagation constant β (1/m)
6 μm	H_{11}	4.70×10^6
	H_{12}	4.68×10^6
8 μm	H_{11}	4.85×10^6
	H_{12}	4.83×10^6

Case 1: Field pattern through coaxial DB waveguide

The radial- and phi-components of the electric field are analyzed through coaxial DB waveguide when considering the outer boundary as $r = 8\,\mu$m. For obtaining the surface plot, the value of ϕ is kept in the range $0 \leq \phi \leq 6.28$ rad. Here for the sake of simplicity, we evaluate two lower-order hybrid modes, H_{11} and H_{12}, and use the allowed values of propagation constant $\beta = 4.85 \times 10^6$ (1/m) and 4.83×10^6 (1/m), respectively.

Figure 2 shows the radial component of the electric field through coaxial optical fiber for different propagation modes. Herein, Fig. 2(a) demonstrates the field pattern of radial component of electric field through dielectric region of the coaxial optical fiber for hybrid mode H_{11}. From this plot, it is observed that electric field decays along the radial direction of the guide. The electric field is maximally concentrated at the lower interface when $r \approx 2.5\,\mu$m, whereas it decreases towards the outer interface of coaxial optical fiber. Next, radial component of the electric field for higher order mode H_{12} is analyzed and depicted in Fig. 2(b). Here, we consider the same parameters as used for Fig. 2(a). The corresponding plot shows that electric field remains maximum at $r \approx 2.75\,\mu$m and minimum at the outer interface. From the plots, we can deduce that electric field remains high for lower order mode H_{11} compared with higher-order mode H_{12}, and this is the result of DB-medium effect.

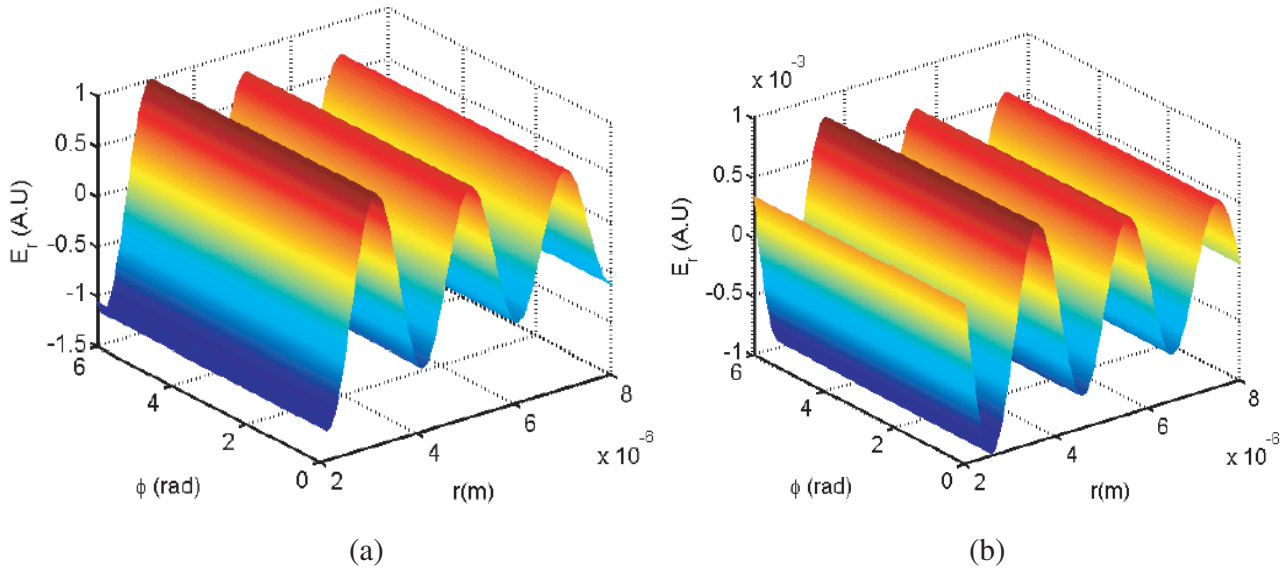

Figure 2. Radial component of the electric field through coaxial optical fiber corresponding to (a) H_{11} mode and (b) H_{12} mode.

Similar to radial component, we discuss the phi-component of the electric field for the propagating modes. In this context, Fig. 3(a) shows phi-component of electric field for H_{11} mode. It is noticed that electric field is negligibly small along phi direction as compared to the respective field along radial direction. Again, the amplitude of phi-component of electric field remains maximum near the inner boundary of the fiber as compared to what we observed in the radial case (for Fig. 2(a)). Next for the

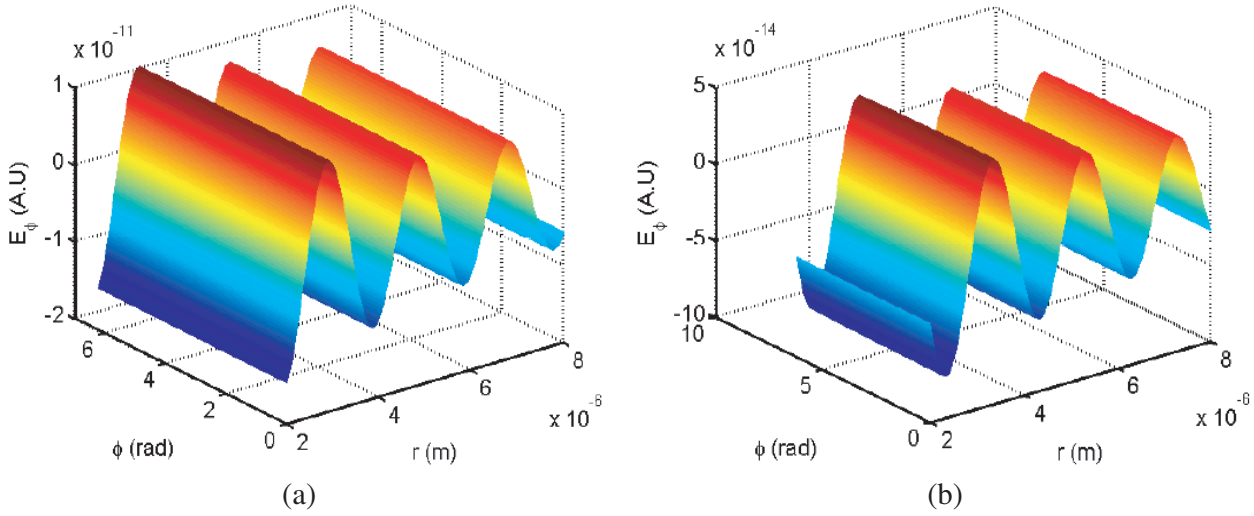

Figure 3. Phi component of the electric field through coaxial optical fiber corresponding to (a) H_{11} mode and (b) H_{12} mode.

case of H_{12} mode phi-component of electric field pattern is shown in Fig. 3(b). Here, we can notice a similar trend again, but amplitude is smaller than all earlier stated situations.

Case 2: Power distribution through coaxial DB waveguide

Now, we consider the power distribution as a function of radius through fiber given in Fig. 1. In this scenario, the power distributions corresponding to two distinct dimensions of the core (when $b = 6$ and $8\,\mu m$) are depicted in Fig. 4. Fig. 4(a) shows the power distribution through coaxial optical fiber when outer radius is taken as $r = 6\,\mu m$. For this purpose, we consider two lower-order hybrid modes H_{11} and H_{12}, and their corresponding propagation constants are $\beta = 4.70 \times 10^6$ and 4.68×10^6, respectively. It is noticed that the power for H_{12} mode remains high in the central region of guide and then decreases gradually towards its outer interface. Similarly, for H_{11} mode case, it decreases monotonically as moving towards inner interface, and the maximum value is obtained near the outer interface at $b = 2.8\,\mu m$. Moreover, when comparing power distribution between these modes, H_{12} mode has shown higher power than H_{11} mode. To the best of our knowledge, this kind of observation has never been noticed before.

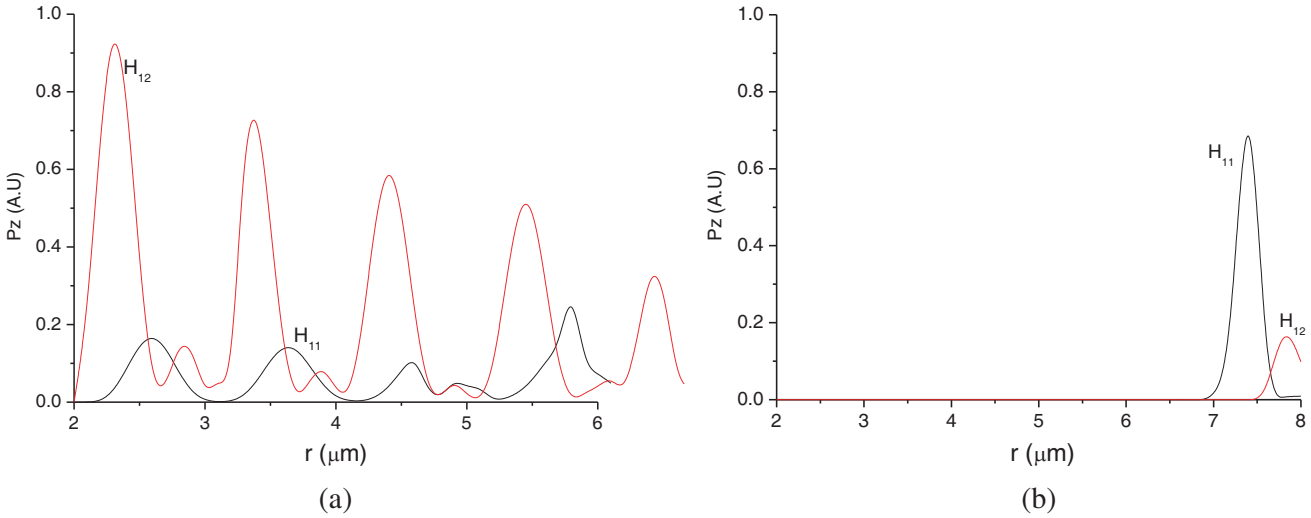

Figure 4. Power through coaxial optical fiber having outer radius (a) $b = 6\,\mu m$ and (b) $b = 8\,\mu m$.

The overall results show that the powers obtained for the lower order hybrid modes are reduced to minimum value near the outer boundary. This phenomenon may arise due to the use of DB boundary.

Now radius of the coaxial optical fiber is increased from 6 μm to 8 μm, and all other parameters values are considered unchanged. The corresponding results are shown in the Fig. 4(b). It is noticed that power confinement is shifted near the outer interface of coaxial optical fiber. In this situation, H_{11} mode occupies higher power than H_{12} mode which is reverse to earlier stated situations. The power at DB interface is decreased sharply due to DB boundary effect. Here we conclude that the use of DB medium along the dimension of the waveguide remains affected in tailoring the confinement through optical fiber.

4. CONCLUSION

In this work, we have presented a numerical solution about the distribution of electric field and power propagation through coaxial optical fiber. Therefore, eigenvalue equation is solved using suitable boundary conditions at the core-clad interface of the transmission medium. From the analysis results, it is noticed that the maximum amplitude of the electric field components through coaxial optical fiber is obtained near the inner DB boundary and decreases gradually towards the outer boundary. In addition, power is confined near the inner boundary of the waveguide and shifted towards the outer interface for larger dimensions. The numerical results show that H_{12} mode has higher power distribution than H_{11} mode due to DB boundary effect when the smaller dimension of the waveguide is considered. Results show that electric field and power pattern may be tailored by altering the radial dimension of coaxial optical fiber.

REFERENCES

1. Smith, D. R., W. J. Padilla, D. C. Vier, S. C. Nemat-Nasser, and S. Schultz, "Composite medium with simultaneously negative permeability and permittivity," *Phys. Rev. Lett.*, Vol. 84, 4184–4187, 2000.
2. Tretyakov, S., A. Sahvola, and L. Jylha, "Backward-wave regime and negative refraction in chiral composites," *Phot. And Nanost.*, Vol. 3, No. 2–3, 107–115, 2005.
3. Chen, J., Y. Yang, and S. Zhung, "Observation of the inverse Doppler effect in negative index materials at optical frequencies," *Nat. Photon.*, Vol. 5, 239–245, 2011.
4. Ginis, V., J. Danckaert, I. Veretennicoff, and P. Tassin, "Controlling Cherenkov radiation with transformation optical metamaterials," *Phy. Rev. Lett.*, Vol. 113, 167402.1–4, 2014.
5. Christensen, J. and F. J. G. de Abajo, "Negative refraction and backward waves in layered acoustic metamaterial," *Phy. Rev. B*, Vol. 86, 024301.1–7, 2012.
6. Monzon, C. and D. W. Forester, "Negative refraction and focusing of circularly polarized waves in optically active media," *Phys. Rev. Lett.*, Vol. 95, 123904.1–4, 2005.
7. Schuring, D., J. J. Mock, B. J. Justice, S. A. Cummer, J. B. Pendry, A. F. Starr, and D. R. Smith, "Metamaterial electromagnetic cloak at microwave frequencies," *Science*, Vol. 314, 977–980, 2006.
8. Zhu, H. and F. Semperlotti, "Metamaterial based embedded acoustic filters for structural applications," *AIP Advances*, Vol. 3, 092121.1–7, 2013.
9. Hummelt, J. S., S. M. Lewis, M. A. Shapiro, and R. J. Temkin, "Design of a metamaterial-based backward-wave oscillator," *IEEE Transactions on Plasma Science*, Vol. 42, 930–936, 2014.
10. Liu, W., Z. N. Chen, and X. Qing, "Metamaterial-based low-profile broadband mushroom antenna," *IEEE Transactions on Antennas and Propagation*, Vol. 62, 1165–1172, 2014.
11. Rhee, J. Y., Y. J. Yoo, K. W. Kim, Y. J. Kim, and Y. P. Lee, "Metamaterial-based perfect absorbers," *Journal of Electromagnetic Waves and Applications*, Vol. 28, No. 13, 1541–1580, 2014.
12. Baqir, M. A. and P. K. Choudhury, "Propagation through uniaxial anisotropic chiral waveguide under DB-boundary conditions," *Journal of Electromagnetic Waves and Applications*, Vol. 27, No. 6, 783–793, 2013.

13. Lindell, I. V. and A. H. Sihvola, "General electromagnetic Boundary conditions involving normal field components," *IEEE Anten. and Wire. Propag. Lett.*, Vol. 8, 877–880, 2009.
14. Lindell, I. V. and A. H. Sihvola, "Electromagnetic boundary conditions defined in terms of normal field components," *IEEE Trans. on Antenn. and Propag.*, Vol. 58, 1128–1135, 2010.
15. Lindell, I. V. and A. H. Sihvola, "Circular waveguide with DB-boundary conditions," *IEEE Trans. on Micro. Theo. and Tech.*, Vol. 58, No. 4, 903–909, 2010.
16. Zaluški, D., D. Muha, and S. Hrabar, "Experimental verification of metamaterial-based DB unit cell," *ELMAR, Proceedings*, 2012.
17. Zaluški, D., S. Hrabar, and D. Muha, "Practicle realization of DB metasurface," *App. Phy. Lett.*, Vol. 104, 234106.1–234106.5, 2014.
18. Lindell, I. V. and A. H. Sihvola, "Electromagnetic boundary conditions and its realization with anisotropic metamaterial," *Phy. Rev. E*, Vol. 79, 026604.1–7, 2009.
19. Baqir, M. A. and P. K. Choudhury, "Waves in coaxial optical fiber under DB-boundaries," *Optik*, Vol. 125, No. 12, 2950–2953, 2014.
20. Khalid, M., A. A. Syed, and Q. A. Naqvi, "Circular cylinder with D'B, DB' and D'B' boundary conditions placed in chiral and chiral nihility media," *Int. J. App. Electromag. and Mech.*, Vol. 44, 59–68, 2014.
21. Hussain, A., S. A. Naqvi, A. Illahi, A. A. Syed, and Q. A. Naqvi, "Fields in fractional parallel plate DB waveguides," *Progress In Electromagnetics Research*, Vol. 125, 273–294, 2012.
22. Hassan, M. H., M. J. Mughal, M. M. Ali, and Q. A. Naqvi, "Electromagnetic fields in a circular waveguide with DB-boundary conditions internally coated with chiral-nihility medium," *Int. J. Applied Electromag. and Mechanics*, Vol. 40, 27–35, 2012.
23. Lindell, I. V. and A. Sihvola, "Soft-and-hard/DB boundary conditions defined by a skewon-axion medium," *IEEE Trans. on Anten. and Propag.*, Vol. 61, No. 2, 768–774, 2013.
24. Zhang, B., H. Chen, B. I. Wu, and J. A. Kong, "Extraordinary surface voltage effect in the invisibility cloack with an active device inside," *Phy. Rev. Lett.*, Vol. 100, 063904.1–4, 2008.
25. Yaghjian, A. D., "Extreme electromagnetic boundary conditions and their manifestation at the inner surfaces of sperical and cylinderical cloaks," *Metamaterials*, Vol. 4, 70–76, 2010.
26. Iqbal, N. and P. K. Choudhury, "On the power distributions in elliptical and circular helically designed chiral nihility core optical fibers," *Journal of Nanophotonics*, Vol. 10, 016008.1–12, 2016.
27. Ghasemi, M. and P. K. Choudhury, "On the sustainment of optical power in twisted clad dielectric cylindrical fibers," *Journal of Electromagnetic Waves and Applications*, Vol. 27, No. 11, 1382–1391, 2013.